

Supporting Information

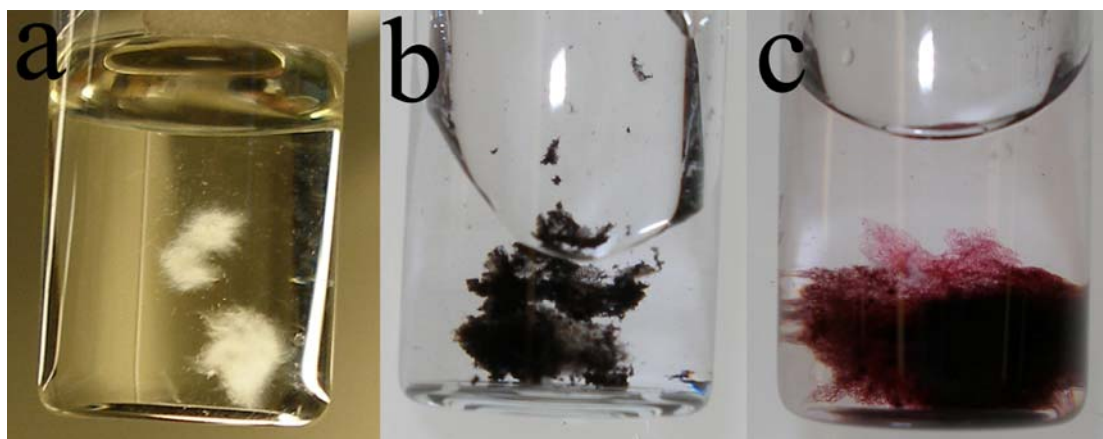


Figure S1, Photographs of (a) PVP jelly-fish like aggregate; (b) PVP-gold aggregate co-assembled from PVP and gold nanoparticles with a high concentration; (c) PVP-gold aggregate co-assembled from PVP and gold nanoparticles with a concentration 5 times lower than that in b.

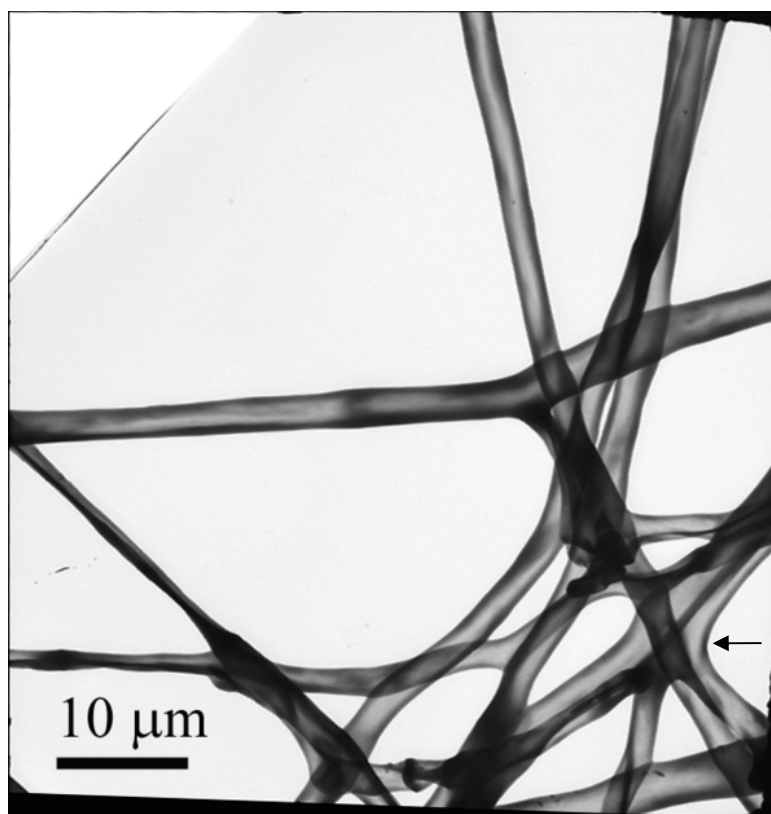
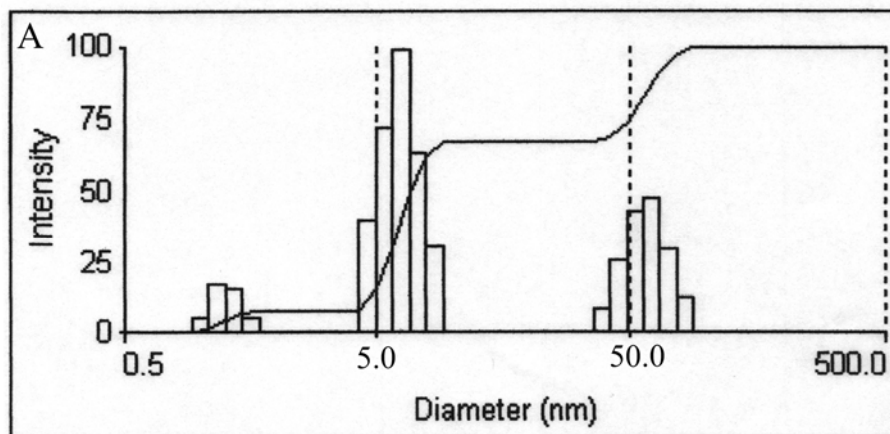
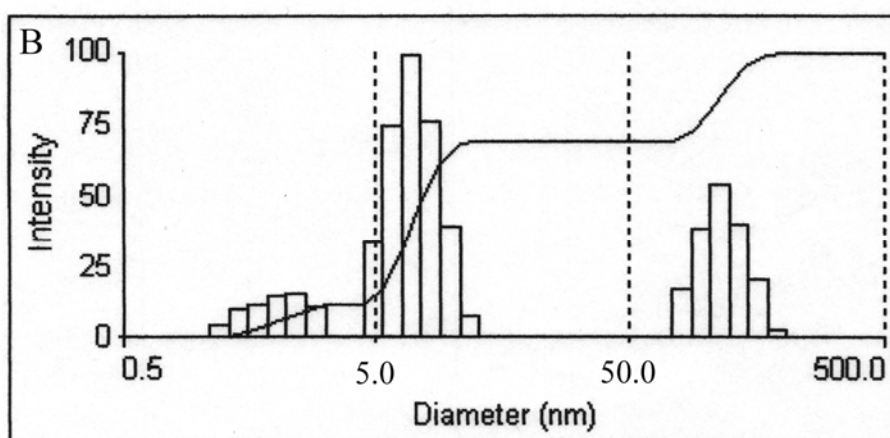


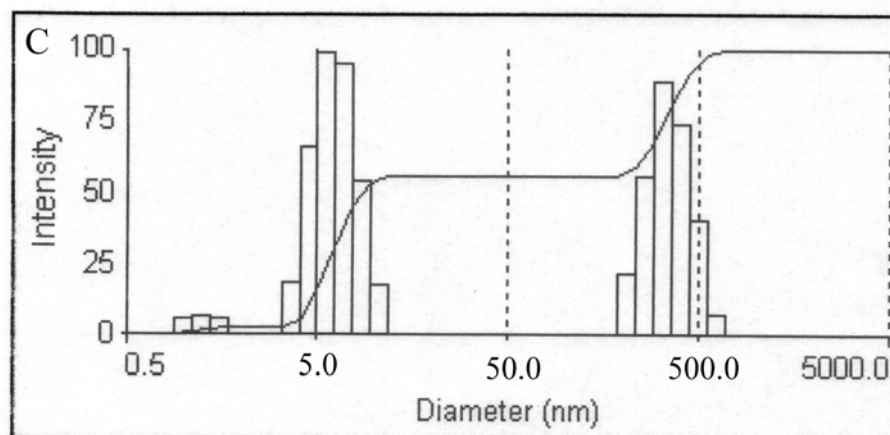
Figure S2, A typical TEM image of PVP hollow fibers. The thickness of fiber wall varies, which can be judged from the nonuniform contrast along the axes. Some segments of the fibers have dark contrast at the magnification shown here, but hollow channels can still be observed from these segments under high brightness electron beam. However, images can hardly be taken due to the lack of stability of PVP fibers under high energy beam. A black arrow shows a hollow junction at the branch.



Multimodal Size Distribution



Multimodal Size Distribution



Multimodal Size Distribution

Figure S3. Particle size distribution in 5.7 wt. % PVP aqueous solution determined by dynamic Light Scattering (DLS) measurement. (A) Freshly prepared solution, (B) Solution aged for 1 day, (C) Solution aged for 4 days. The mean diameters for these three time points are 22.0 nm, 39.0 nm and 156.6 nm, respectively. The particles of around 5 nm are corresponding to the individual polymer chains (M.W. 10 kDa). The particles around 50 nm or larger are corresponding to the aggregates formed as a result of the self-assembly of polymer chains.

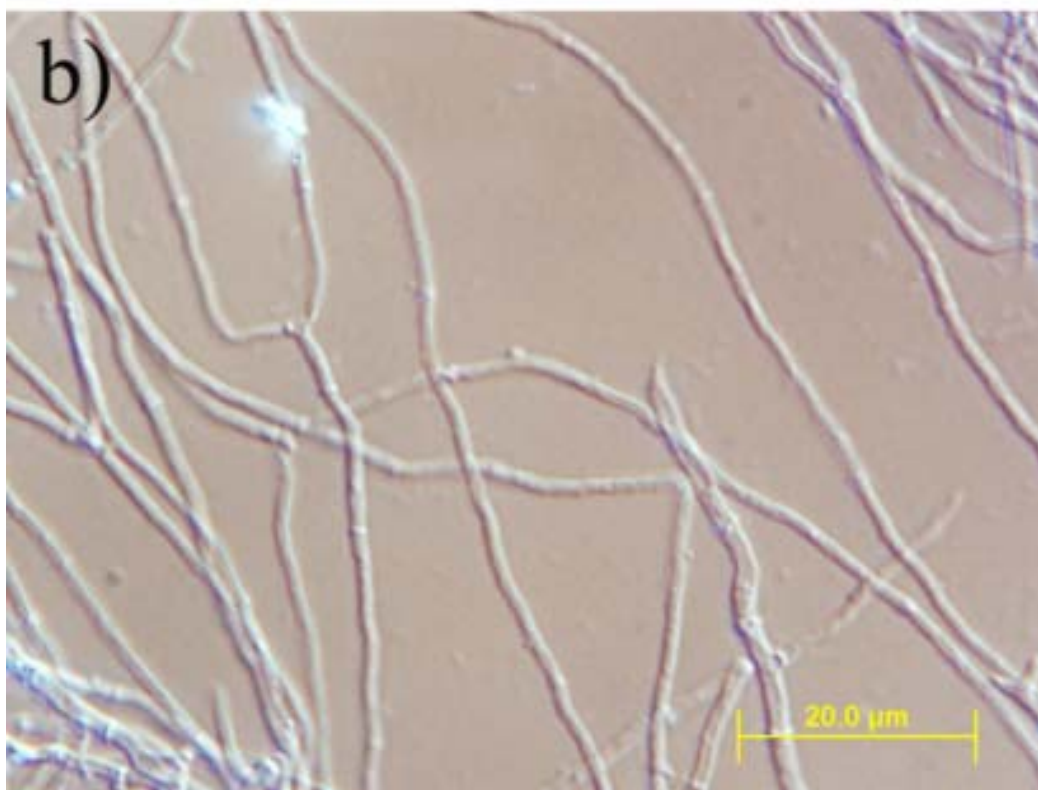


Figure S4 PVP fibers imaged directly in the solution phase under optical microscope. (a) Fibers which are formed at the early stage and later become the core (Fig.2). The image shows that the fibers were initially formed as a result of the aggregation of PVP microspheres and appeared to be pearl-necklace-like chains. (b) Fibers formed at later stage and outgrown from the core (see Fig. S1-a). The outgrown fibers have a smoother surface, indicating that outgrowth occurs through the assembly of free PVP molecules in the solution onto the end of pearl-necklace-like chains, rather than through the continuous aggregation of PVP microspheres.

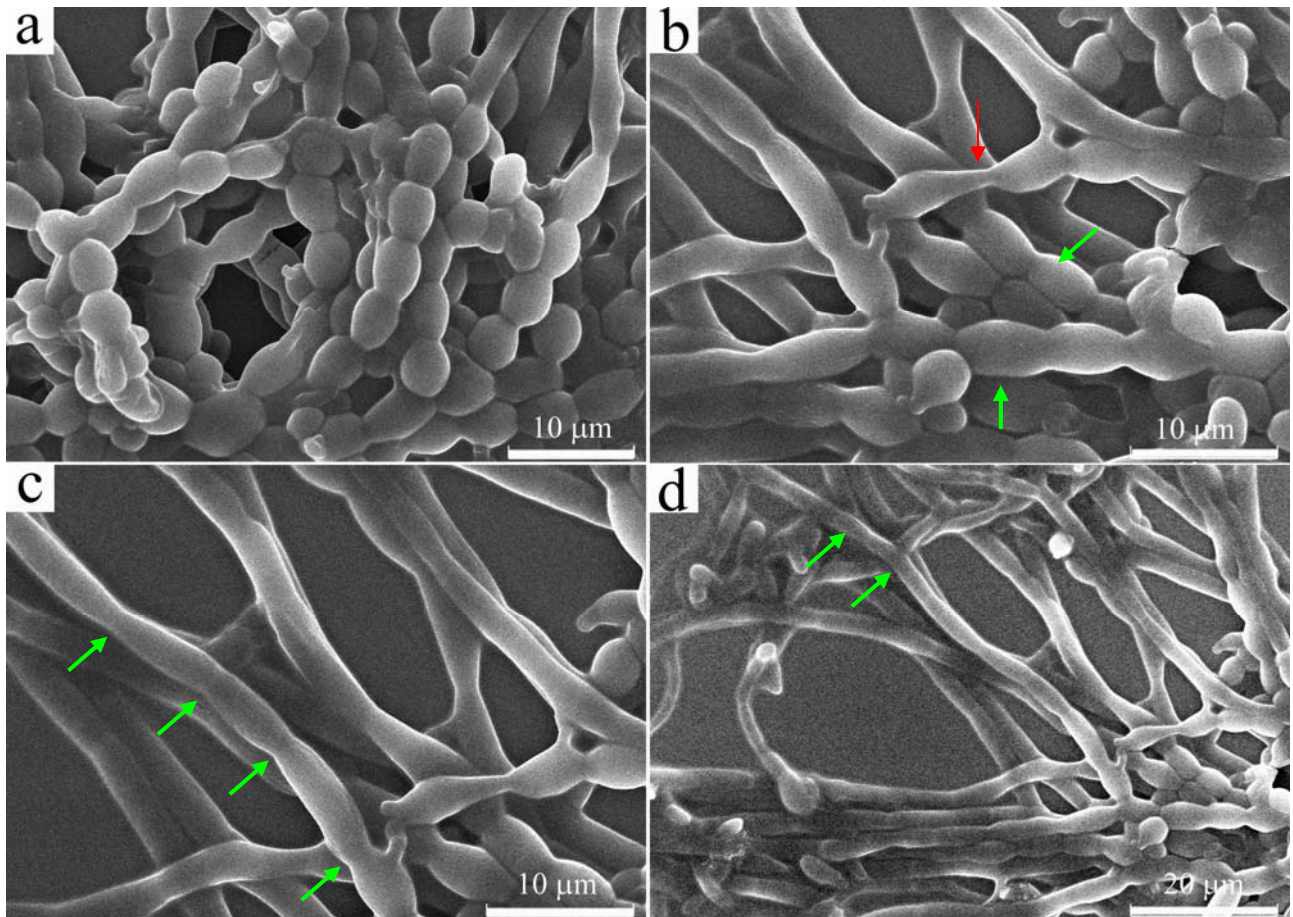


Figure S5, A continuous morphological transition of PVP microspheres at the end of pearl-necklace-like chains. (a) At the center of the chain (same image as Fig. 2b in the text); (b) Slightly away from the center, spheres became ellipsoids (green arrows), red arrow shows an ellipsoid further elongating into rods; (c) further away, ellipsoids became rods, green arrows show the junction of each rods; (d) rods finally transitioned into smooth hollow fibers (green arrows) at even further distance from the central chains. (b-d) were imaged at the same fiber but different spots of interest.

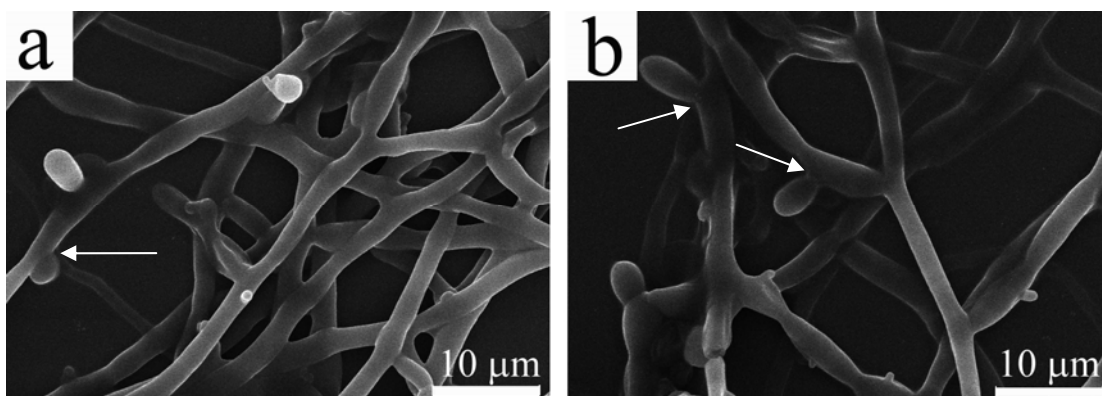


Figure S6, SEM images showing the early stage of branch formation. (a) A PVP microsphere highlighted by an arrow that has just settled onto the sidewall of a fiber and a PVP branch may grow from this microsphere; (b) Branches indicated by arrows that have grown longer.

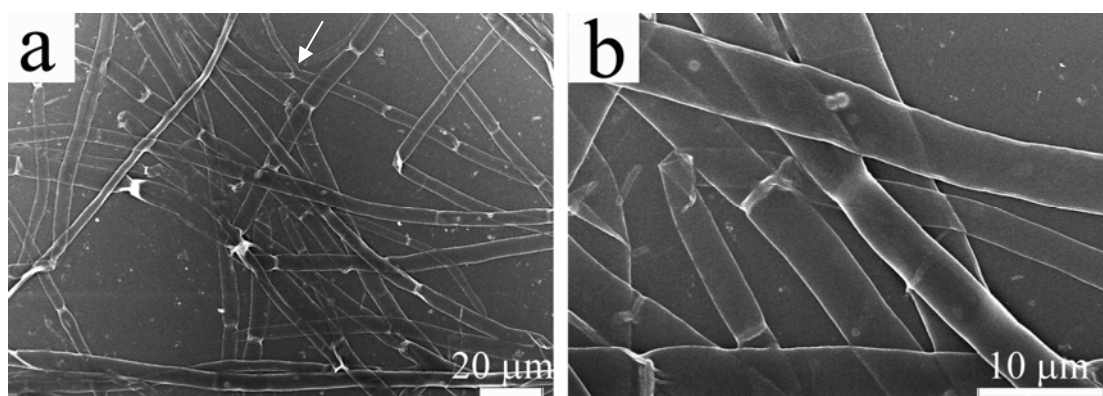


Figure S7, SEM images of fibers resulted from the self-assembly of PVP with a molecular weight of 40 kDa. Compared to PVP with a lower molecular weight (10 kDa), their average diameter had been increased from 2-3 μm to around 5 μm . (a) Low magnification; (b) Higher magnification. A branched structure is highlighted by an arrow in (a). It should be noted that the aggregate has been sonicated to get isolated fibers for imaging purpose and during this process the branches may be separated from the stems.

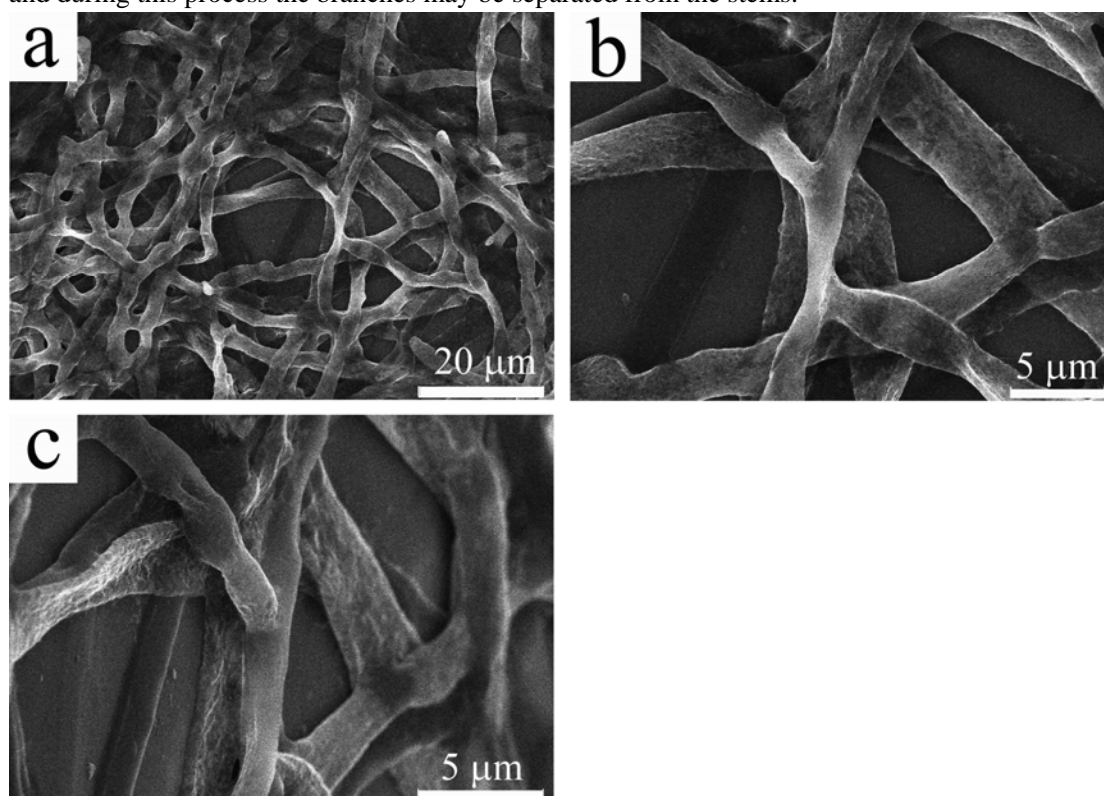


Figure S8, SEM images of PVP-gold fibers, co-assembled from the solution, in which the gold nanoparticles concentration was 5 times lower (Fig. S1-c). (a) Low magnification View; (b) higher magnification view showing branches of the fibers; (c) A 60° tilted view of b.